Journal of Alloys and Compounds 643 (2015) S178–S181

Contents lists available at ScienceDirect

Journal of Alloys and Compounds

journal homepage: www.elsevier.com/locate/jalcom

# Precipitation hardening in the Cu–11 wt.%Al–10 wt.%Mn alloy with Ag addition

R.A.G. Silva [a,*], A. Paganotti [a], A.T. Adorno [b], C.M.A. Santos [b], T.M. Carvalho [b]

[a] Departamento de Ciências Exatas e da Terra, UNIFESP, Diadema, SP, Brazil
[b] Departamento de Físico-Química, UNESP, Araraquara, SP, Brazil

ARTICLE INFO

*Article history:*
Available online 8 January 2015

*Keywords:*
Metals and alloys
Phase transitions

ABSTRACT

In this work the precipitation hardening in the Cu–11 wt.%Al–10 wt.%Mn alloy with Ag addition was studied using different experimental techniques. The results indicated that the hardening on ageing of the Cu–11 wt.%Al–10 wt.%Mn alloy is only due to bainite precipitation, while in the Cu–11 wt.%Al–10 wt.%Mn–3%Ag alloy three reactions in sequence can occur, including the bainite precipitation.



## 1. Introduction

Copper-based alloys are widely used in many fields because of their good combination of high thermal and electrical conductivities. In particular, Cu-based alloys with high performance are required in field of electronic materials, such as substrate and lead frame in printed board, and interconnection, because the electronic packaging has a tendency to miniaturisation [1]. The Cu–Al–Mn alloys are quite interesting, since it can show shape memory effect [2] and magnetic effects [3], depending on the Mn and Al contents. Below approximately 773 K the Cu–Al–Mn alloys have the ordered structure $L2_1$ (bcc), which transforms martensitically to 3R-fcc, 18R (small martensite plates) or 2H (large martensite plates) structures. Ageing of Cu–Al–Mn SMAs is a very complex process due to the possibility of formation of different phases, and also can lead to volume changes because during the transition from martensite to austenite the lattice transforms from hexagonal or rhombohedral symmetry to body centred cubic crystal structure, depending on the Mn composition [4]. Phase transformations as bainitic-type also can be observed. In this case, it can interfere on shape memory effect and hardening of alloy. In this paper the effect of Ag addition on precipitation hardening of the Cu–11 wt.%Al–10 wt.%Mn alloy was investigated using microhardness measurements with time, differential scanning calorimetry (DSC), scanning electron microscopy (SEM) with an energy dispersive X-ray microanalyser (EDX), and magnetic measurements (MM).

## 2. Materials and methods

The Cu–11 wt.%Al–10 wt.%Mn and Cu–11 wt.%Al–10 wt.%Mn–3 wt.%Ag alloys were prepared in an arc furnace under argon atmosphere using 99.95% copper, 99.97% aluminium, 99.98% silver and 99.95% manganese as starting materials. The samples were annealed during 120 h at 1123 K for homogenisation and after annealing they were maintained at 1123 K for 1 h and quenched in water. The Vickers microhardness measurements were made with a HMV-2T Microhardness Tester-SHIMADZU using a load of 9.8 N. Scanning electron micrographs were obtained in a FEI Inspect F50 – High Resolution microscopy with energy dispersive X-ray microanalyser (EDX). The DSC curves were obtained using a DSC Q20 TA Instruments with heating rate of 10 K $min^{-1}$, argon flux of 50 mL/min and Pt pan. The magnetic properties were measured using a vibrating-sample magnetometer (VSM) at 300 K.

## 3. Results and discussion

Fig. 1(a and b) show the plots of microhardness change with ageing time obtained for the Cu–11 wt.%Al–10 wt.%Mn and Cu–11 wt.%Al–10 wt.%Mn–3 wt.%Ag alloys. The starting points of these ones correspond to samples quenched from 1123 K in water. From Fig. 1a and similar curves obtained for the Cu–11 wt.%Al–10 wt.%Mn–3 wt.%Ag alloy, it is possible to observe that all curves showed an incubation period which decreases with the increase of the temperature, and a peak hardness for all temperatures. The incubation period and peak hardness values are shifted to higher hardness values with the addition of Ag (see Fig. 1b), suggesting a change in the microstructure of this alloy. In order to analyse the ageing of the Cu–11 wt.%Al–10 wt.%Mn–3 wt.%Ag alloy, DSC curves were obtained from samples aged at 473 K in different times, as shown in Fig. 1c. The starting points of these curves were ascribed to the phases formed after the ageing at 473 K in the time ranges cited in Fig. 1c.

* Corresponding author.
*E-mail address:* galdino.ricardo@gmail.com (R.A.G. Silva).

http://dx.doi.org/10.1016/j.jallcom.2014.12.208
0925-8388/

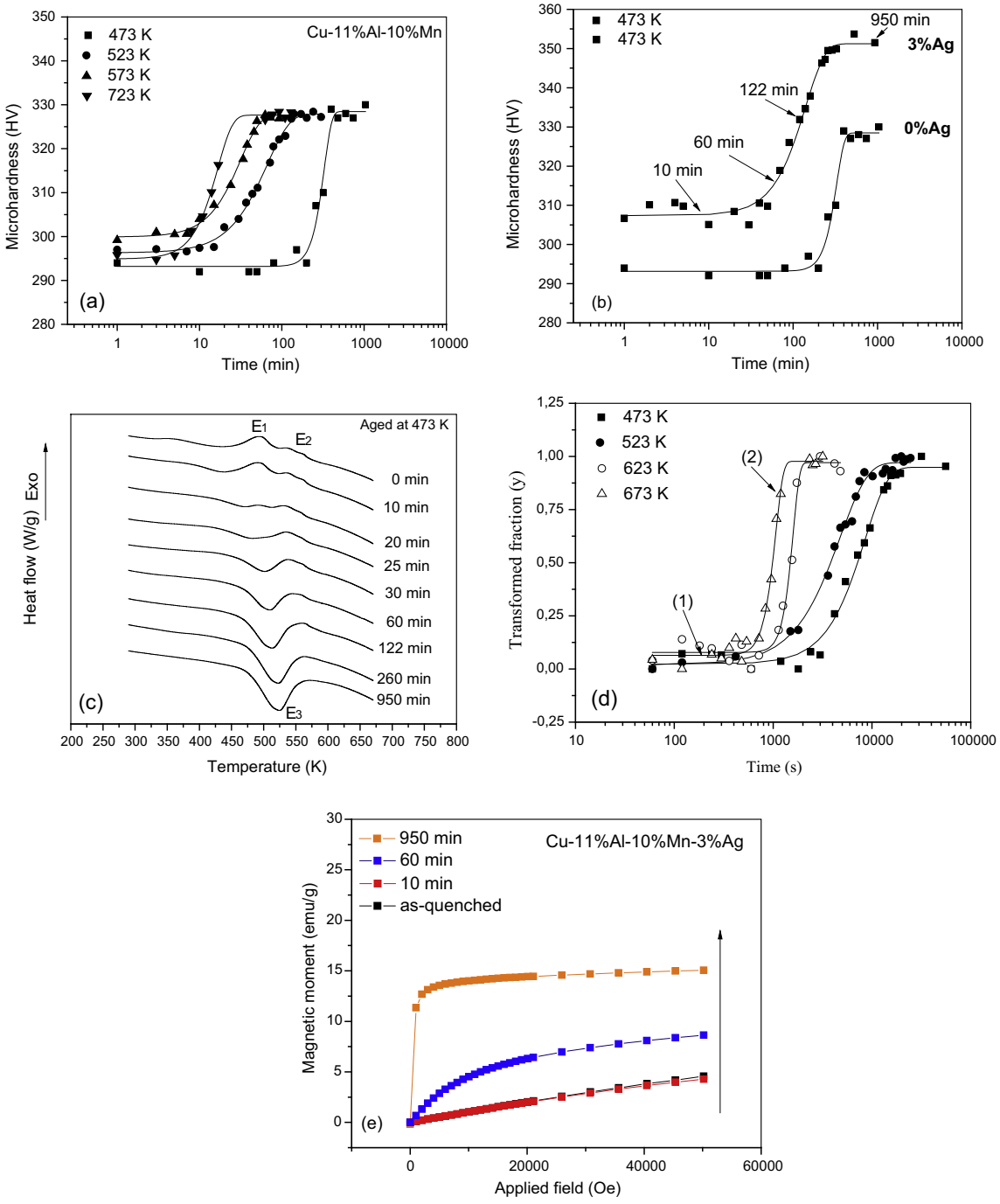


**Fig. 1.** (a) Microhardness curves with time obtained for the Cu–11 wt.%Al–10 wt.%Mn alloy, (b) microhardness curves with time obtained for the Cu–11 wt.%Al–10 wt.%Mn and Cu–11 wt.%Al–10 wt.%Mn–3 wt.%Ag alloys, (c) DSC curves obtained for the Cu–11 wt.%Al–10 wt.%Mn–3 wt.%Ag alloy after ageing at 473 K in different times, (d) plots of transformed fraction with time obtained for the Cu–11 wt.%Al–10 wt.%Mn–3 wt.%Ag alloy and (e) magnetic moment curves vs. applied field obtained for samples aged in different times at 473 K.

In Fig. 1c the reference curve obtained before the ageing (*curve for* 0 min) shows two thermal events. The exothermic event $E_1$ is associated with α phase precipitation [5] and it was not detected in the curve obtained for the Cu–11 wt.%Al–10 wt.%Mn alloy. The event $E_2$ was attributed to the bainite formation [6]. With increase of ageing time these thermal events disappear and a new peak $E_3$ is verified from 30 min and it becomes more intense with increase of ageing time for the Cu–11 wt.%Al–10 wt.%Mn–3 wt.%Ag alloy. The latter is due to the decomposition reaction, $L2_{1(f)} + DO_3 \rightarrow L2_{1(p)}$ [7]. These results indicate that during ageing of the Cu–11 wt.%Al–10 wt.%Mn–3 wt.%Ag alloy three reactions in sequence can occur in the temperature and time ranges studied. Firstly, α phase precipitation is concluded in the early step, after the bainite precipitation continues up to the end of microhardness increase and then the $L2_{1(p)}$ phase decomposition reaction formed during quenching is finished. In the maximum of ageing curves the $L2_{1(f)}$, $DO_3$ and bainitic phases are presented in the Cu–11 wt.%Al–10 wt.%Mn–3 wt.%Ag alloy. Fig. 1e shows the magnetic moment curves with applied field obtained for the Cu–11 wt.%Al–10 wt.%Mn–3 wt.%Ag alloy after ageing at 473 K in different times. These times were chosen from Fig. 1b. The curves show a marked increase in the magnetisation saturation with the

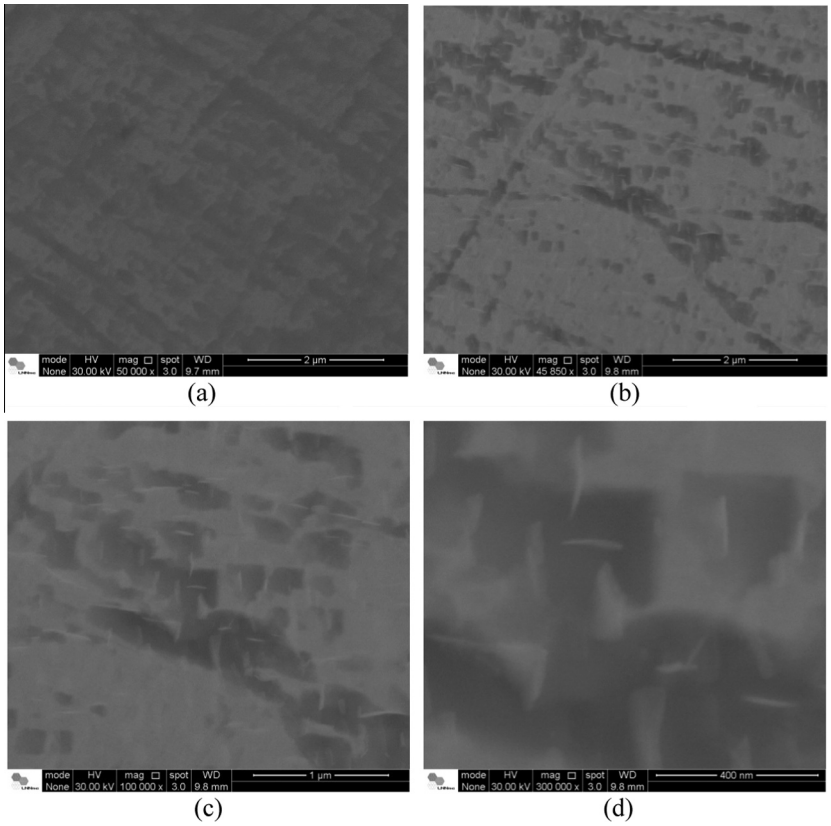


**Fig. 2.** Scanning electron micrographs (SEM) obtained for the Cu–11 wt.%Al–10 wt.%Mn–3 wt.%Ag alloy after ageing at 673 K for (a) 180 s and (b–d) 1200 s.

**Table 1**
Kinetics parameters obtained for the Cu–11 wt.%Al–10 wt.%Mn alloy.

| $T$ (K) | 473 | | 523 | | 573 | | 723 | | $Ea$ (kJ mol$^{-1}$) |
|---|---|---|---|---|---|---|---|---|---|
| Parameters | $n$ | $k$ (s$^{-1}$) | $n$ | $k$ (s$^{-1}$) | $n$ | $k$ (s$^{-1}$) | $n$ | $k$ (s$^{-1}$) | (51.0 ± 2.4) |
| Values | 2.0 | $4.72 \times 10^{-5}$ | 1.7 | $2.55 \times 10^{-4}$ | 1.6 | $5.31 \times 10^{-4}$ | 2.0 | $4.70 \times 10^{-3}$ | |

**Table 2**
Kinetics parameters obtained for the Cu–11 wt.%Al–10 wt.%Mn–3 wt.%Ag alloy.

| $T$ (K) | 473 | | 523 | | 623 | | 673 | | $Ea$ (kJ mol$^{-1}$) |
|---|---|---|---|---|---|---|---|---|---|
| Parameters | $n$ | $k$ (s$^{-1}$) | $n$ | $k$ (s$^{-1}$) | $n$ | $k$ (s$^{-1}$) | $n$ | $k$ (s$^{-1}$) | (28.3 ± 0.4) |
| Values | 1.5 | $1.13 \times 10^{-4}$ | 1.5 | $2.16 \times 10^{-4}$ | 5.0 | $6.37 \times 10^{-4}$ | 4.8 | $9.42 \times 10^{-4}$ | |

increase of the ageing time, which is related to the increase of the $L2_{1(f)}$ phase relative fraction, thus confirming that during the ageing the $L2_{1(p)} \rightarrow L2_{1(f)} + DO_3$ decomposition reaction [7] is occurring in this alloy. For the Cu–11 wt.%Al–10 wt.%Mn alloy bainitic precipitation is dominant, suggesting that higher ageing times are needed for the total decomposition of the $L2_{1(p)}$ phase at this temperature.

Fig. 2 shows the SEM images obtained for the Cu–11 wt.%Al–10 wt.%Mn–3 wt.%Ag alloy after ageing at 673 K for 180 s and 1200 s, as indicated in Fig. 1d by the arrows 1 and 2, respectively. In Fig. 2a no precipitate was observed, but when the ageing time was increased some of them were observed (Fig. 2b). In Fig. 2c and d these precipitates are evidenced, with mean size at about 100–200 nm. EDX analyses showed that the precipitates are rich in Cu, while dark regions in Fig. 2(c and d) has higher Al fraction. This suggests that after the initial formation of α phase, the precipitates probably grow by a diffusion mechanism. Ag-rich precipitates were not observed with SEM analyses in the temperature and time ranges considered. Fig. 1d shows the plots of the transformed fraction as a function of the ageing time obtained from microhardness curves with time of the Cu–11 wt.%Al–10 wt.%Mn–3 wt.%Ag alloy. Similar curves were obtained for the Cu–11 wt.%Al–10 wt.%Mn alloy. Considering that the reactions observed show nucleation and growth after an incubation period, the kinetic process may be described by the Johnson–Mehl–Avrami–Kolmogorov (JMAK) equation [8],

$$y = 1 - \exp[-(kt)^n] \quad (1)$$

which can be rewritten as

$$\ln[-\ln(1-y)] = n \ln k + n \ln t \quad (2)$$

Tables 1 and 2 show the values of $n$ and $k$ obtained from fit of Eq. (2) to the experimental points in Fig. 1d and in similar curves found for the Cu–11 wt.%Al–10 wt.%Mn alloy. The analysis of the $n$ values obtained for the Cu–11 wt.%Al–10 wt.%Mn alloy indicates a

diffusion controlled growth with all shapes growing from small dimensions and decreasing nucleation rate ($1½ \leqslant n \leqslant 2½$). For the Cu–11 wt.%Al–10 wt.%Mn–3 wt.%Ag alloy the $n$ values indicate a diffusion controlled growth with all shapes growing from small dimensions with zero nucleation rate ($n = 1½$) at 473 and 523 K, and increasing nucleation rate ($n > 2½$) at 623 and 673 K [9]. These $n$ values confirm that in the Cu–11 wt.%Al–10 wt.%Mn alloy there is only one process, while in the Cu–11 wt.%Al–10 wt.%Mn–3 wt.%Ag alloy at least two processes are presented. This confirms the discussion proposed for Fig. 1b and c.

Considering the Arrhenius equation,

$$k = k_o \exp(-Q/RT) \quad (3)$$

and the $k$ values showed in Tables 1 and 2, the activation energies for the reactions can be estimated from the slope of the plots of $\ln k$ vs. $1/T$. The obtained values are showed in Tables 1 and 2. For the Cu–11 wt.%Al–10 wt.%Mn alloy the activation energy was $Q = (51.0 \pm 2.4)$ kJ mol$^{-1}$, close to the value ($Q \cong 60$ kJ mol$^{-1}$) obtained by Sutou et al. for bainite precipitation in the $Cu_{71.9}Al_{16.6}Mn_{9.3}Ni_2B_{0.2}$ alloy [8]. This difference between the activation energy values can be attributed to the change of Al content. For the Cu–11 wt.%Al–10 wt.%Mn–3 wt.%Ag alloy a lower value was determined. This activation energy value shows that the presence of Ag increases the bainitic reaction rate. The increase in the bainitic precipitation rate suggests that Ag atoms can be occupying the Cu sites in the phase structures. This effect can be related to the saturation of the metallic matrix with the silver atoms dissolved during quenching, that can cause a stability decrease in the alloy phases due to the increase of lattice stresses, thus decreasing the temperature in which the $L2_{1(p)}$ phase decomposition occurs and promoting an increase in fraction of Cu atoms available to form the bainitic phase. These effects can be associated with increase in the bainitic phase formation rate in the Cu–11 wt.%Al–10 wt.%Mn–3 wt.%Ag alloy.

## 4. Conclusions

The results indicated that the dominant reaction on ageing of the Cu–11 wt.%Al–10 wt.%Mn alloy is bainite precipitation, while in the Cu–11 wt.%Al–10 wt.%Mn–3 wt.%Ag alloy three reactions in sequence can occur. Firstly, α phase precipitation is concluded in the early step, after the bainite precipitation continues up to end of microhardness increase and then the $L2_{1(p)}$ phase decomposition reaction formed during the quenching is concluded. In the maximum of ageing curves obtained for the Cu–11 wt.%Al–10 wt.%Mn–3 wt.%Ag alloy the $L2_{1(f)}$, $DO_3$ and bainitic phases are dominant. The presence of silver increases the bainitic precipitation rate.

## Acknowledgments

The authors thank to FAPESP and CNPq for the financial support and LNNano for technical support during electron microscopy work (FEI Inspect F50 – High Resolution SEM).

## References

[1] H.N. Soliman, N. Habib, Effect of ageing treatment on hardness of Cu–12.5 wt.%Al shape memory alloy, Indian J. Phys, http://dx.doi.org/10.1007/s12648-014-0480-z.
[2] Y. Zheng, C. Li, F. Wan, Y. Long, Cu–Al–Mn alloy with shape memory effect at low temperature, J. Alloys Comp. 441 (2007) 317–322.
[3] L. Yiping, A. Murthy, G.C. Hadjipanayis, Giant magnetoresistance in Cu–Mn–Al, Phys. Rev. B 54 (5) (1996) 3033–3036.
[4] A. Mielczarek, N. Kopp, W. Riehemann, Ageing effects after heat treatment in Cu–Al–Mn shape memory alloys, Mater. Sci. Eng. A 521–522 (2009) 182–185.
[5] R.A.G. Silva, A. Paganotti, L. Jabase, A.T. Adorno, T.M. Carvalho, C.M.A. Santos, Ag-rich precipitates formation in the Cu–11%Al–10%Mn–3%Ag alloy, J. Alloys Comp. 615 (2014) S160–S162.
[6] L.G. Bujoreanu, S. Stanciua, P. Barsâñescub, N.M. Lohana, Study of the transitory formation of $\alpha_1$-bainite, as a precursor of α-phase in tempered SMAs, in: IV. Proc. of SPIE Advanced Topics in Optoelectronics, Microelectronics, and Nanotechnologies, vol. 7297, 2009, 72970B-1, <http:// dx.doi.org/10.1117/12.823620>.
[7] M. Bouchard, G. Thomas, Phase transitions and modulated structures in ordered $(Cu–Mn)_3Al$ alloys, Acta Mettall. 23 (1975) 1485–1500.
[8] Y. Sutou, N. Koeda, T. Omori, R. Kainuma, K. Ishida, Effects of ageing on bainitic and thermally induced martensitic transformations in ductile Cu–Al–Mn-based shape memory alloys, Acta Mater. 57 (2009) 5748–5758.
[9] J.W. Christian, The Theory of Transformations in Metals and Alloys Part 1, third ed., Pergamon Press, Oxford, 2002.